Am J Transl Res 2022;14(3):1578-1591
www.ajtr.org /ISSN:1943-8141/AJTR0133425

Original Article

REDD1 gene knockout alleviates vascular smooth muscle cell remodeling in pulmonary hypertension

Xiaoyu Fang, Min Xie, Xiansheng Liu, Yuanzhou He

Department of Respiratory Diseases, NHC Key Laboratory of Respiratory Diseases, Department of Respiratory and Critical Care Medicine, Tongji Hospital, Tongji Medical College, Huazhong University of Sciences and Technology, 1095 Jiefang Avenue, Wuhan 430030, Hubei, China

Received March 23, 2021; Accepted January 17, 2022; Epub March 15, 2022; Published March 30, 2022

Abstract: Objectives: Regulated in development and DNA damage responses 1 (REDD1) is an important transcription factor regulating mitochondria homeostasis, which is the important pathological alteration of pulmonary hypertension (PH). However, it is unclear whether REDD1 regulates the PASMCs mitochondria homeostasis by the similar mechanism in pulmonary arterial remodeling induced by hypoxia. Methods: The global REDD1-knockout rats (REDD1-KO) on Sprague-Dawley background were used to generate a chronic hypoxia model of PH. Right ventricular hypertrophy and vascular remodeling were detected after exposure to hypoxia. Additionally, proliferation, apoptosis, migration, mitochondria homeostasis, and autophagy were performed *in vivo* and *in vitro*. Results: The current research found that in human and experimental rats of PH, REDD1 expression is upregulated in the PASMCs. REDD1 gene knockout alleviated hypoxia PH and hemodynamic changes effectively and reversed hypoxic pulmonary vascular remodeling. In addition, REDD1 knockdown reduces the impairment of mitochondrial function caused by hypoxia in HPASMCs via autophagy inhibition, and this process may be regulated through the Parkin gene. Moreover, REDD1 knockdown can effectively inhibit the proliferation and migration of hypoxic PASMCs, and induce their apoptosis *in vivo* and *in vitro*. Conclusions: Our results suggested that REDD1 might be a potential target for improved pulmonary vascular remodeling in PH.

Keywords: REDD1, PASMCs, pulmonary hypertension, vascular remodeling

Introduction

Pulmonary hypertension (PH) is a severe pulmonary vascular disease characterized by remodeling of the distal Pulmonary artery. Clinically, PH is mainly manifested by continuous and significantly increased pulmonary pressure, which eventually leads to right ventricular failure and death [1]. PH is a common complication of a variety of respiratory diseases, including COPD, asthma and interstitial pulmonary disease, which seriously affect the prognosis of the disease. The median survival of COPD patients with severe PH is less than 3 years [2]. At present, although the study on the pathogenesis of PH has made some progress, it has not been fully clarified, and the clinical treatment has not achieved good efficacy. Therefore, it is of great practical significance to actively explore the pathogenesis of PH for the discovery of effective therapeutic targets.

Mitochondrial homeostasis plays an important role in the occurrence and development of PH pulmonary artery remodeling [3]. Any changes in mitochondrial homeostasis will affect the energy metabolism of cells and lead to the imbalance of proliferation and apoptosis. Mitochondrial homeostasis plays an important role in intracellular homeostasis and cell survival under stress. Studies have shown that hypoxia induces apoptosis tolerance of pulmonary artery smooth muscle cells (PASMCs) by changing mitochondrial intimal permeability [4]. Compared with the normal control group, mitochondria in PASMCs of PH patients were deformed, swollen significantly, and obviously in a state of depolarization [5]. When dichloroacetate was applied to alter the mitochondrial depolarization state of PASMCs, it was found that pH and pulmonary artery remodeling could be significantly alleviated [6]. In addition, stud-

ies have confirmed that mitochondrial dysfunction may be involved in pulmonary artery remodeling through redox imbalance leading to pulmonary hypertension.

Regulated in Development and DNA Damage Responses 1 (REDD1), also known as RTTP801/DIG1, located at 10q24.33, is a key stress regulation gene in cells under hypoxic, energy deficit and multiple DNA damage stress environments. At the same time, more and more evidence shows that REDD1 is also a regulatory gene of mitochondrial homeostasis. It was found that inhibition of REDD1 expression in fibroblasts significantly reduced ROS production in mitochondria, and the structure and function of mitochondria were significantly disordered. Under the same conditions, overexpression of REDD1 significantly increases ROS production and mitochondrial homeostasis [7]. In addition, studies have shown that REDD1 negatively regulates Akt, which is involved in regulating mitochondrial function by inhibiting the release of mitochondrial cytochrome C and downstream Pim-1 and FoxO1. REDD1 improves insulin sensitivity in pancreatic beta cells by regulating mitochondrial homeostasis [8]. REDD1 can also induce autophagy by inhibiting mTOR (mammalian target of rapamycin) signaling pathway, participate in mitochondrial quality control and maintain mitochondrial homeostasis, thereby promoting stress survival of various tumor cells [9].

Our previous study found that hypoxia can induce autophagy, and after autophagy is inhibited, hypoxia leads to abnormal proliferation of PASMCs, apoptosis tolerance and obvious reversal of migration [10]. The main purpose of this study was to establish a hypoxic PH model using REDD1 gene knockout rats, to study the role of REDD1 in the pathogenesis of PH, and to explore its possible mechanism.

Materials and methods

Ethics statement

All of the studies were approved by the Huazhong University of Science and Technology Committee, the Tongji Medical College Ethics Committee at Tongji Hospital (Approval number: 20170881700051) and performed according to NIH guidelines.

Experiment animal models

The global REDD1-knockout rats (REDD1-KO) on a Sprague-Dawley background were generated by Cyagen Inc. (Jiangsu, China). In brief, the exon 1 to exton 3 were selected to be knocked out. The gRNA targeting vectors were constructed and confirmed by sequencing. The gRNA vectors and Cas9 mRNA generated by in vitro transcription were co-injected into fertilized eggs and finally we got three rats. After about 8 weeks, the rats were bred to get homozygous.

The male REDD1-KO or REDD1-wildtype (REDD1-WT) rats were exposed to 21% oxygen (normoxia) or 10% oxygen (hypoxia) in the chamber for 8 h per day. The Oxygen concentration was maintained by the Oxycycler Model A84 (BioSpherix, USA). All the animals were housed in a 12-hour light/dark cycle and had access to standard rat chow and water. The experiment was approved by the Ethics Committee of Tongji Hospital, Tongji Medical College, Huazhong University of Science and Technology.

Hemodynamic measurements

Four weeks later, rats were anesthetized with pentobarbital injection (120 mg/kg ip). The right jugular vein was exposed in supine position. A 1.2-Fr pressure catheter (GuGeSheng-Wu, Wuhan, China) assisted by guide wire was inserted to the right jugular vein and positioned in the right ventricle. The guide wire was pulled out and the pressure transductor was connected to the catheter. The right ventricular systolic pressure (RVSP) was recorded using Power Lab Software (ADI instrument, Australia). Subsequently, the right carotid artery was exposed to detect the systemic blood pressure of the rats.

Evaluation right ventricular hypertrophy

The rats were euthanized, and the hearts were separated to the right ventricle (RV) and left ventricle plus septum (LV+S). The weight ratio of RV to LV+S was calculated to define the degree of right ventricular hypertrophy.

Immunohistochemistry (IHC) and immunofluorescence (IF)

Immunohistochemical staining was performed on the lung sections by using routine protocols.

Briefly, sections were blocked with 5% BSA for 1 h at room temperature and incubated at 4°C overnight with anti-REDD1 (1:50), anti-α-SMA (1:100), anti-LC3 (1:100) and anti-P62 (1:100) at 4°C overnight. These slides were then treated with second antibody for 1 h at room temperature. For IHC, color reaction was applied by using 3, 3'-diaminobenzidine tetrachloride (DAB) chromogen solution. For IF, the nuclei were stained by DAPI. Finally, the slides were covered and observed under microscope.

Transmission electron microscope (TEM)

The lung tissues and cells were fixed in 2.5% glutaraldehyde phosphate-buffered saline (pH 7.4) for 24 h at room temperature. Subsequently, the samples were fixed in 1% osmium tetroxide for 2 h. The samples were embedded in epoxy resin after the dehydration. Finally, the specimens were cut into 60 nm sections and the sections were stained with lead citrate. Ultrathin sections were examined with a TEM (PhilipsEM420).

Western blot analysis

The lysate from lung tissue or cells were collected and centrifuged at 12,000 rpm for 15 min to obtain supernatant. SDS-PAGE (polyacrylamide gel electrophoresis) was applied to separate the proteins and the proteins were transferred to 0.22-μm microporous polyvinylidene difluoride membranes. Membranes were blocked with 5% nonfat milk for 1 h at room temperature and incubated within primary antibodies: REDD1 (1:1000), Bax (1:1000), Bcl2 (1:1000), MMP9 (1:1000), LC3 (1:1000), and P62 (1:1000) overnight at 4°C. The chemiDoc detection system (Bio-Rad, Hercules, USA) was used to detect the bands and the results were quantified by ImageJ software.

RNA isolation and quantitative PCR analysis

Total RNAs were extracted from cells using TRIzol (Invitrogen, US). Reverse transcription was applied with a Prime Script RT Reagent Kit (TaKaRa Bio, China) following the manufacture instructions. Gene expression was evaluated using the SYBR-Green (Biorad, US). The β-actin mRNA was used as an internal control. The sequences of the primers are as follows: β-actin forward 5'-AGAAAATCTGGCACCACACCT-3' and reverse 5'-GATAGCACAGCCTGGATAGCA-3'; REDD1 forward 5'-GCTTAGGGGCCAACAAGG-3' and reverse 5'-TCTGGATGTCACACCACTGTT-3'.

Cell proliferation assay

Cells were planted in 96-well plates (3000/well). After transfecting with si-RNA, the cells were exposed to normoxia or hypoxia for 24 h. Cell proliferation was determined by Edu and CCK8 assay according to the manufacturer's instructions. Absorbance at 450 nm was measured by ELx800 Universal Microplate Reader (Bio-Tek, USA). The cells stained with Edu were imaged under the fluorescence microscope (Olympus, Japan).

Cell apoptosis assay

Cells were harvested by centrifugation and washed twice with cold PBS. Then the cells were suspended in 500 μl of binding buffer. 5 ul FITC and PI solutions were added to the tube and incubated for 20 min at room temperature in dark, followed by analysis with a FACS flow cytometer (Mindray, China). The percentage of Q2 and Q4 was used to estimate the cell apoptosis.

Migration assay

Migration was measured using transwell chamber. Cells transfected with si-RNA were digested and enumeberated. 200 ul cell suspension with 10,000 cells was seeded in the upper chamber, and 600 ul medium was added into the low chamber. After exposing to normoxia or hypoxia for 24 h, the upper medium was replaced with medium containing 1% FBS, and the lower with 15%. Cells were fixed with 4% paraformaldehyde for 15 min and stained with crystal violet for 30 min. Cotton swabs were used to remove the cells on the upper surface of the membrane. The numbers of migration cells were quantified with the light microscope (Nikon, Japan).

Small interfering RNA (siRNA)

REDD1 and negative control siRNAs were purchased from RiboBio (Guangzhou, China). Si-REDD1 (50 nM) and si-NC (50 nM) was transfected into HPASMCs using Lipofectamine 3000 Reagent (Invitrogen, USA). The medium was replaced with new culture medium after

24 h. The sequence of si-REDD1 was as follows: AGACACGGCTTACCTGGAT.

Statistical analysis

Results are shown as the mean ± standard deviation. Statistical differences were determined using Student's t test or one-way analysis of variance (ANOVA). Statistical analyses were performed with GraphPad Prism (GraphPad Software, USA). A value of $P<0.05$ was considered significant.

Results

High levels of REDD1 are expressed in PH patients and hypoxic rats

In order to determine the role of REDD1 in PH, we performed immunohistochemistry staining in the tissues of patients with PH and hypoxic PH rats. REDD1 positive cells located in the pulmonary arteries were prominently increased in PH patients (**Figure 1A**) and hypoxic rats (Figure S1A). REDD1 protein levels were much higher in pulmonary vascular homogenates of hypoxic rats (**Figure 1B**). Consistently, immunofluorescence observation revealed that the expression of REDD1 was highly induced in the medial layer of pulmonary arteries of hypoxic rats, which mainly consists of smooth muscle cells (**Figure 1C**). Moreover, the protein and mRNA expression of REDD1 were detected in HPASMCs exposed to different hypoxia time. The protein level of REDD1 was upregulated under hypoxia, while the mRNA level was also increased and peaked at 18 h (Figure S1B and S1C).

Knockout of REDD1 attenuates hypoxia induced PH

Hemodynamic evaluation showed that the right ventricular systolic pressure (RVSP) of REDD1-KO group was significantly reduced compared with the REDD1-WT group after hypoxia (**Figure 2A**). The right ventricular hypertrophy, assessed by the ratio of right ventricular (RV) weight to left ventricular (LV) plus septum weight (RV/LV+S) and the ratio of RV and body weight (BW), was significantly lower in REDD1-KO rats than that in REDD1-WT rats when exposed to hypoxia condition (**Figure 2B** and **2C**). No difference was observed in systemic arterial blood pressure (BP) and left ventricular ejection fraction among the four groups (**Figure 2D** and **2E**).

REDD1 deficiency alleviates hypoxic pulmonary artery remodeling

The HE staining indicated that hypoxia-induced increase in pulmonary artery wall thickness was decreased in REDD1-KO rats (**Figure 3A**). Furthermore, REDD1-KO rats also exhibited marked decreases of the medial wall thickness compared with REDD1-WT rats (**Figure 3B**). EVG and Masson staining showed that muscularization of distal pulmonary arterioles was prominently lower in REDD1-KO rats than that in the REDD1-WT group following hypoxia exposure (**Figure 3C** and **3D**). These data suggest that REDD1 knockout contributes to the pulmonary artery remodeling in rats.

REDD1 knockdown reduces the impairment of mitochondrial function caused by hypoxia in HPASMCs

High-resolution TEM of hypoxic HPASMCs revealed mitochondrial damage as indicated by loss of cristae and presence of swollen mitochondria, while REDD1 knockdown could partly restore the damage (**Figure 4A**). The total ROS accessed by DCFH-DA assay and H_2O_2 increases caused by hypoxia were downregulated by the transfection of si-REDD1 (**Figure 4A-C**). The MMP was evaluated by TMRM and JC-1. Compared with the si-NC group, the MMP was significantly decreased in si-REDD1 group in HPASMCs exposed to hypoxia (**Figure 4A**). In addition, the ATP assay indicated that si-REDD1 ameliorated the hypoxia induced ATP decrease (**Figure 4A**). Taken together, these results show that the knockdown of REDD1 reduces the impairment of mitochondrial function caused by hypoxia in HPASMCs.

REDD1 deficiency suppresses hypoxia-induced autophagy in vivo and in vitro

The TEM of lung tissues of rats showed that the autophagic vacuoles per cells were much higher in REDD1-KO rats compared with REDD1-WT rats in hypoxia (**Figure 5A**). The increase of ration of LC3II to LCI protein and P62 induced by hypoxia was reduced by REDD1 knockout (**Figure 5B**). Consistently, the IHC of LC3II and P62 also indicated that REDD1 knockout could restore hypoxia induced autophagy in vivo (**Figure 5C**).

In the in vitro assays, the role of REDD1 on the autophagy of HPASMCs was examined using si-

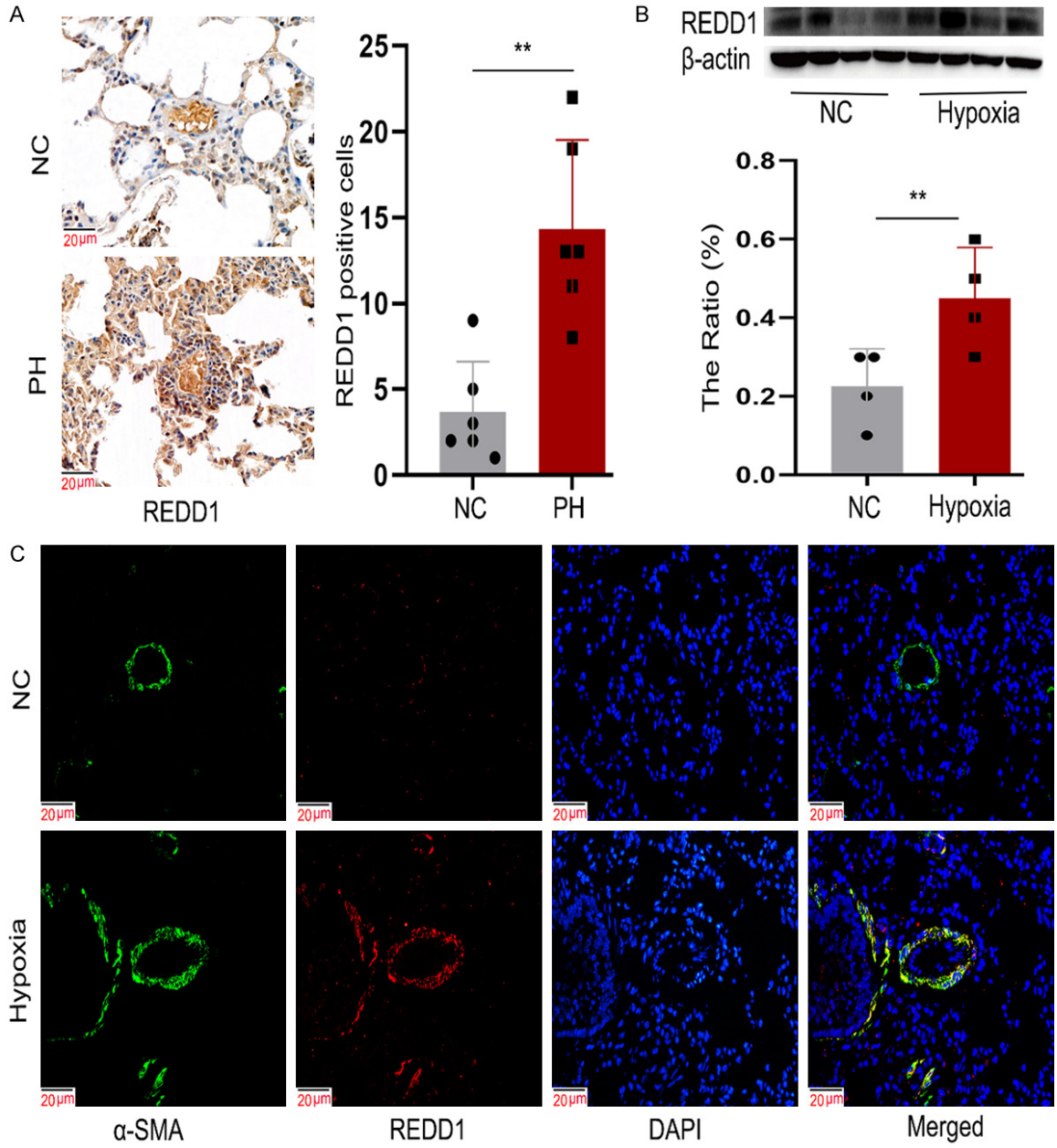

Figure 1. Expression of REDD1 is increased in PH patients and rats. A. Representative images (400×) of REDD1 expression in lung tissues of control (n=6) and PH patients (n=6). B. Western blot analysis and quantification of REDD1 protein levels in lung homogenates of rats exposed to normoxia (21% oxygen) or hypoxia (10% oxygen) for 4 weeks (n=4 for per group). C. The representative fluorescence images of α-SMA and REDD1, expression in lung sections of rats in each group. Nuclei were labeled with DAPI. $^{*}P$ value <0.05, $^{**}P$ value <0.01.

REDD1. The efficiency of si-REED1 was confirmed in protein and mRNA levels (Figure S2). The increases induced by hypoxia in the numbers of autophagic vacuoles in HPASMCs were attenuated by transfecting with si-REDD1 (**Figure 6A** and **6B**). Furthermore, hypoxia upregulated the ration of LC3II to LCI and downregulated P62 protein expression, which indicated the enhancement of autophagy, but si-REDD1 suppressed the increases in HPASMCs (**Figure 6C**).

Moreover, we also investigated the effect of silencing REDD1 on classical autophagy regulatory pathways, mTOR, Pink and Parkin, and we found that si-REDD1 had no effects on the

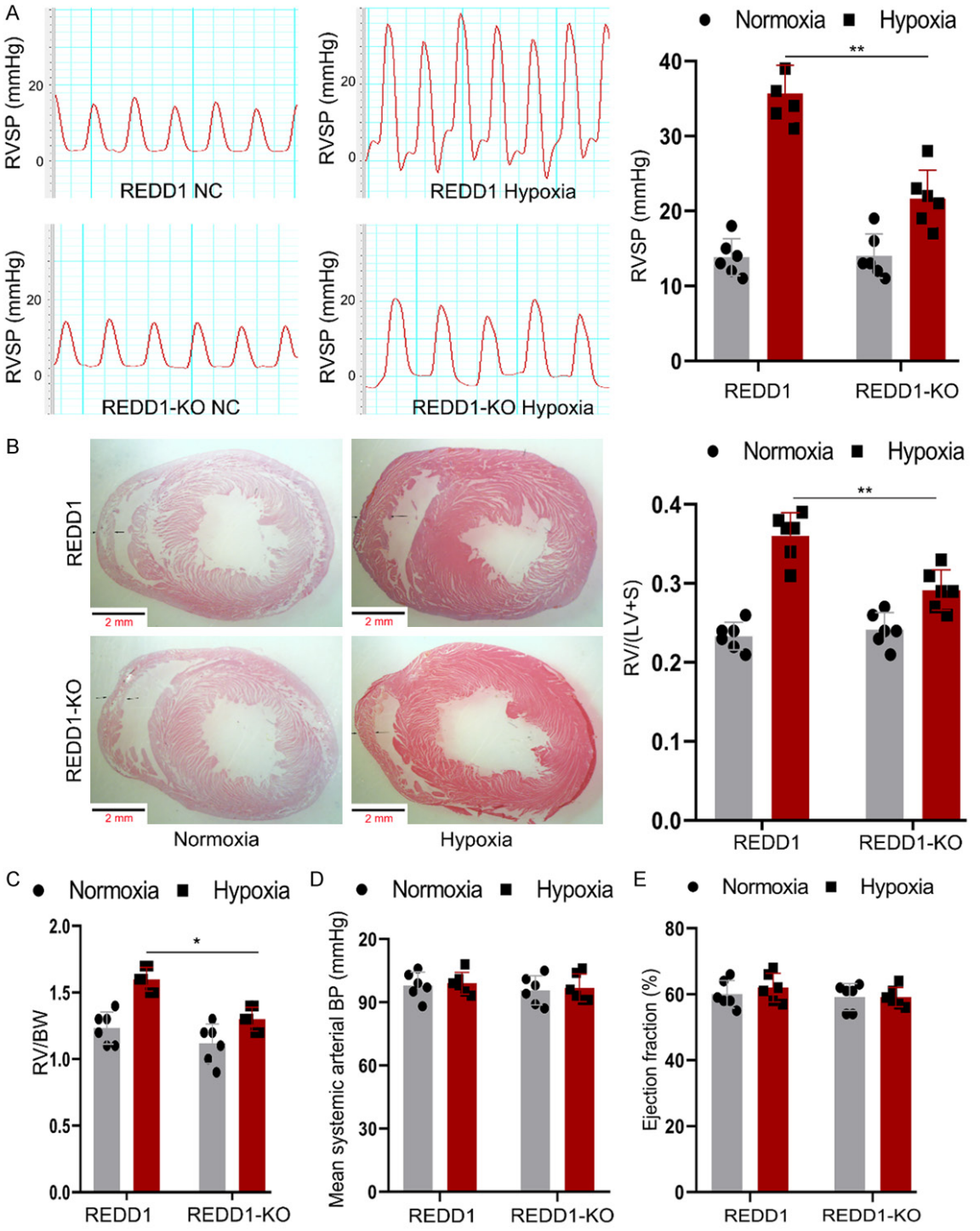

Figure 2. REDD1 deficiency in rats inhibits the development of hypoxia-induced PH. (A) RVSP was measured and quantified in the WT and REDD1-KO rats exposed to normoxia or hypoxia for 4 weeks. (B) Representative HE staining images of ventricle and RV hypertrophy evaluated by the weight ratio of RV/(LV+S). (C) Quantification of the ration of RV to body weight (BW). (D) Mean arterial blood pressure (BP) and (E) left ventricle ejection fraction. n=6 for per group. $^{*}P$ value <0.05, $^{**}P$ value <0.01.

mTOR and Pink. However, REDD1 deletion significantly reversed the expression of hypoxia on Parkin (Figure S3). Furthermore, co-immunoprecipitation assay was used to test the

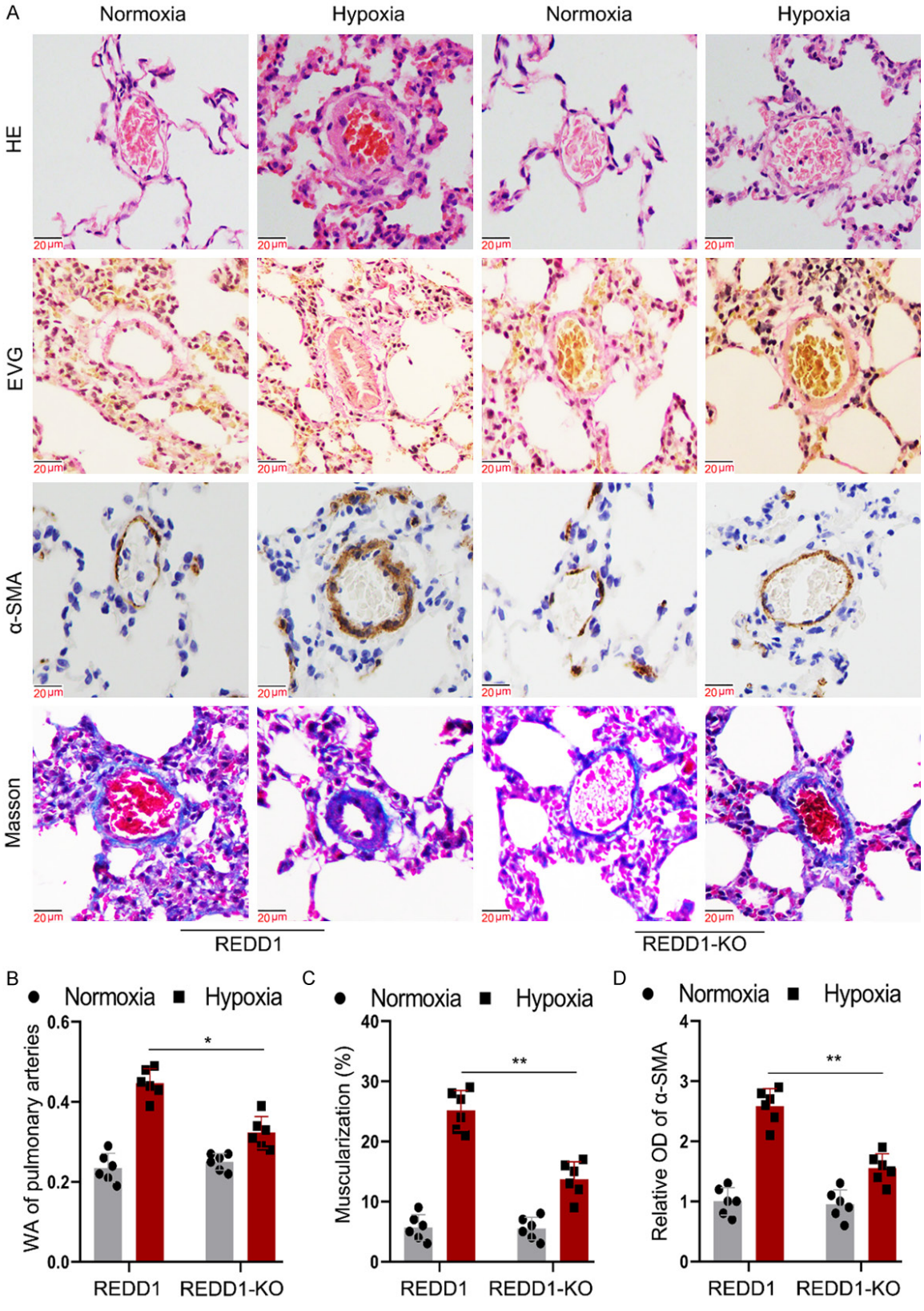

Figure 3. REDD1 knockout attenuates hypoxic pulmonary vascular remodeling. A. Representative images of HE, EVG, α-SMA and Masson staining from WT and REDD1-KO rats' lung under normoxia or hypoxia condition. B. The wall thickness of pulmonary arterioles was calculated. C. Percentage of muscular distal pulmonary vessels. D. Optical density of α-SMA. n=6 per group. $^{*}P$ value <0.05, $^{**}P$ value <0.01.

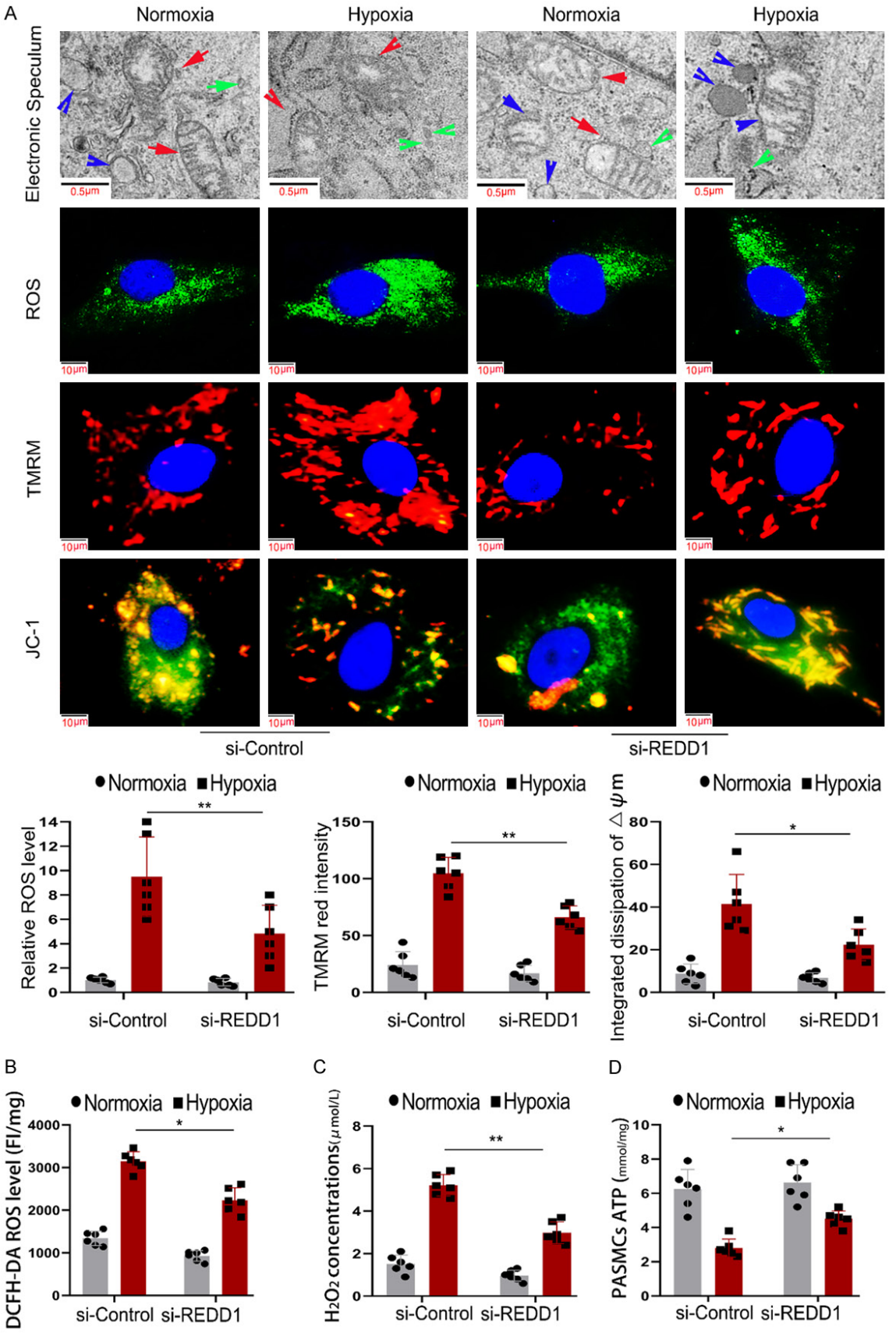
A
Normoxia
Hypoxia
Normoxia
Hypoxia
Electronic Speculum
ROS
TMRM
JC-1
si-Control
si-REDD1
Normoxia Hypoxia
Relative ROS level
TMRM red intensity
Integrated dissipation of △ψm
B
DCFH-DA ROS level (FI/mg)
C
H2O2 concentrations(μmol/L)
D
PASMCs ATP (mmol/mg)

Figure 4. REDD1 knockdown reduces dysfunction of mitochondrial induced by hypoxia in HPASMCs. (A) The morphology of mitochondria was observed by the transmission electron microscope. The ROS was stained by DCFH-DA. The mitochondrial membrane potential (Δψm) was determined by TMRM and JC-1. The representative images were shown and the fluorescence intensity was measured. (B) Analysis of the concentration of ROS. (C) H_2O_2, and (D) ATP in each group of HPASMCs. n=6 per group. $^{*}P$ value <0.05, $^{**}P$ value <0.01. Red arrow: mitochondria; Blue arrow: vesicles; Green arrow: dense body.

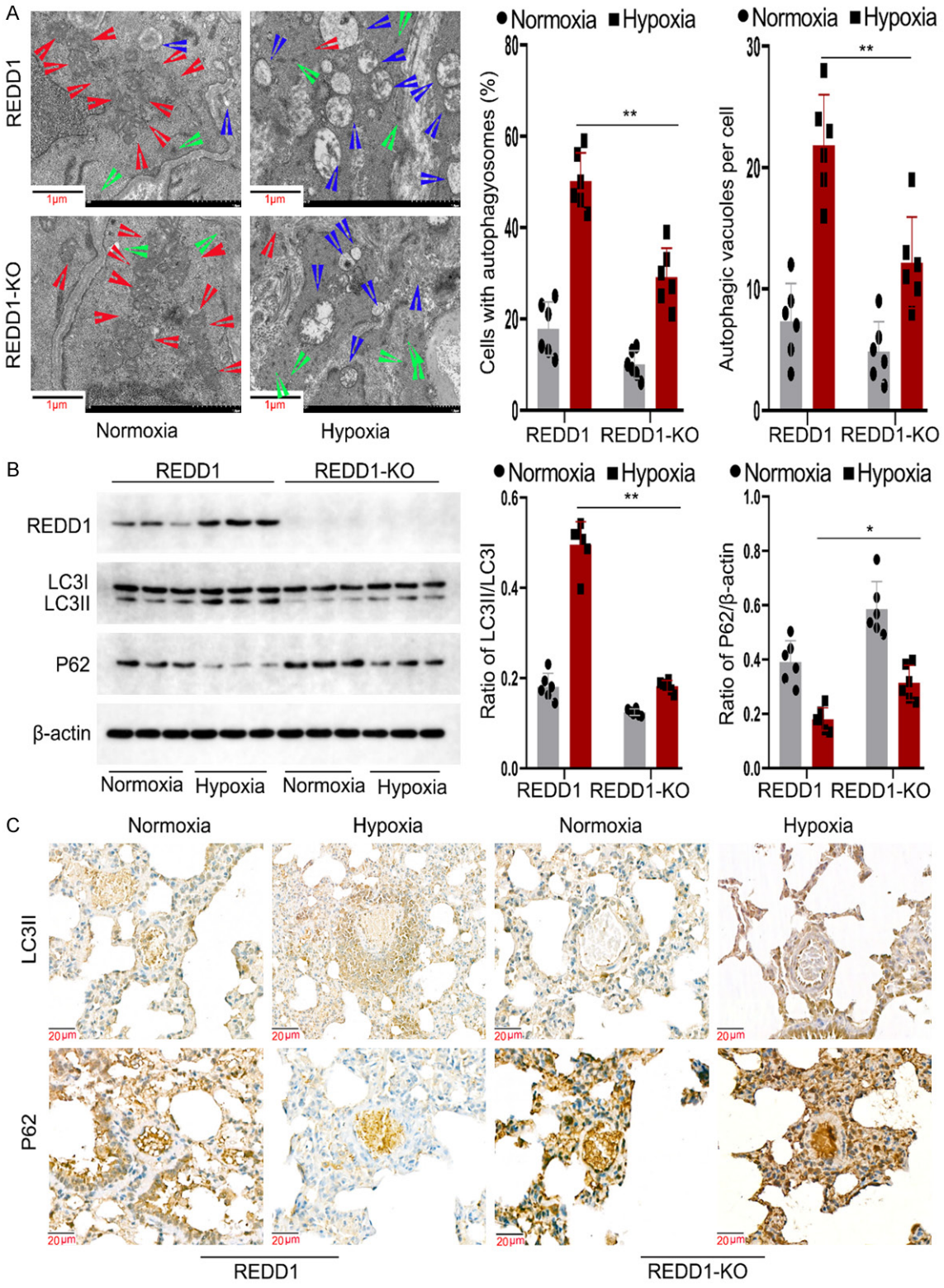

Figure 5. Knockout of REDD1 suppresses hypoxia-induced autophagy in rats. A. The transmission electron microscope was used to observe the alteration of autophagy in rat's lung tissues, and the percentage of cells with autophagosomes and numbers of the autophagic vacuoles per cell were calculated. B. Western blot analysis of LC3 and P62 protein levels in lung homogenates of REDD1-WT and REDD1-KO rats exposed to normoxia or hypoxia for 4 weeks. The ratio of LC3II to LC3I and P62 to β-actin were identified. C. Expression of LC3 and P62 protein of lung sections. n=6 per group. $^{*}P$ value <0.05, $^{**}P$ value <0.01. Red arrow: mitochondria; Blue arrow: vesicles; Green arrow: dense body.

relationship between REDD1 and Parkin in HPASMCs. In addition, our results confirmed that REDD1 and Parkin interacted directly in HPASMCs (Figure S4).

REDD1 knockdown inhibits the proliferation and migration of HPASMCs and induced apoptosis in hypoxic HPASMCs

Given the fact that PASMC proliferation and resistance of apoptosis are crucial for the progress of PH, we investigated the marker for cell proliferation and apoptosis in lung section of rats. As shown in **Figure 7A** and **7B**, the numbers of Ki67 positive cells were reduced in REDD1-KO rats compared with REDD1-WT rats in hypoxia. TUNEL staining indicated that the decreased apoptosis of PASMCs in distal pulmonary arterioles caused by hypoxia in distal pulmonary arterioles was restored by REDD1 knockout (**Figure 7C** and **7D**).

The Edu staining and CCK8 proliferation assay showed that proliferation of HPASMCs transfected with si-REDD1 was significantly reduced compared with the si-NC group in hypoxia (Figure S5A). The percentage of apoptotic cells was much higher in si-REDD1 group than si-NC group in hypoxic HPASMCs (Figure S5B). The results indicated that the migrated cells were prominently decreased by si-REDD1 in HPASMCs exposed to hypoxia (Figure S5C). Moreover, hypoxia increased the SURVIVIN and MMP9 expression and decreased the ratio of BAX to BCL2 in HPASMCs, but REDD1 siRNA inhibited the alteration (Figure S6). These findings indicate that REDD1 regulates the imbalance of proliferation, apoptosis and migration of HPASMCs under hypoxia condition.

Discussion

Through the hypoxic rat PH model, consistent with our previous results, the WT rat model showed higher pulmonary artery pressure, right ventricular hypertrophy, and obvious pulmonary small arteries remodeling. However, the pathological changes in REDD1 knockout rats were partially reversed. In addition, PASMCs in vitro demonstrated that REDD1 knockout inhibited hypoxic-induced autophagy and reversed hypoxic-mitochondrial dysfunction. Furthermore, REDD1 knockdown can inhibit the migration and proliferation of hypoxic PASMCs cells, and promote their apoptosis. Taken together, we hypothesize that REDD1 maintains mitochondrial homeostasis by promoting hypoxic autophagy, leading to migration, proliferation and apoptosis tolerance of PASMCs, thus playing an important role in the pathogenesis of PH (Figure S7).

REDD1 is the target gene of the hypoxia inducible factor 1α (HIF-1α) gene. Our previous studies have confirmed that hypoxic up-regulation of HIF-1α is involved in the regulation of pulmonary artery remodeling [11]. However, there are few reports on the relationship between REDD1 and hypoxic pulmonary artery remodeling. Mitochondrial function is mainly associated with ROS release; studies have shown that REDD1 is closely related to mitochondrial function and hypoxic pulmonary artery reconstruction, which is associated with hypoxia leading to change in mitochondrial ROS. Therefore, REDD1 also referred to as the DNA damage induced by transcription factor 4 (DNA damage inducible transcript, 4 DDIT4). Studies have shown that the content of REDD1 in mitochondria accounts for more than 10% of the total cell volume. Moreover, REDD1 can regulate mitochondrial homeostasis by regulating the release and activity of mitochondrial ROS. In the study of osteosarcoma, the activation of autophagy by the REDD1/TXNIP complex is involved in the regulation of increased mitochondrial ROS release [12]. In breast cancer studies, HIF-1α regulates the increase of ROS release in tumor cells through a negative feedback regulation pathway formed by the REDD1 pathway [13]. Consistent with previous research results, we found that low oxygen leads to increase in the number of mitochondria increased obviously in the PASMCs, divided

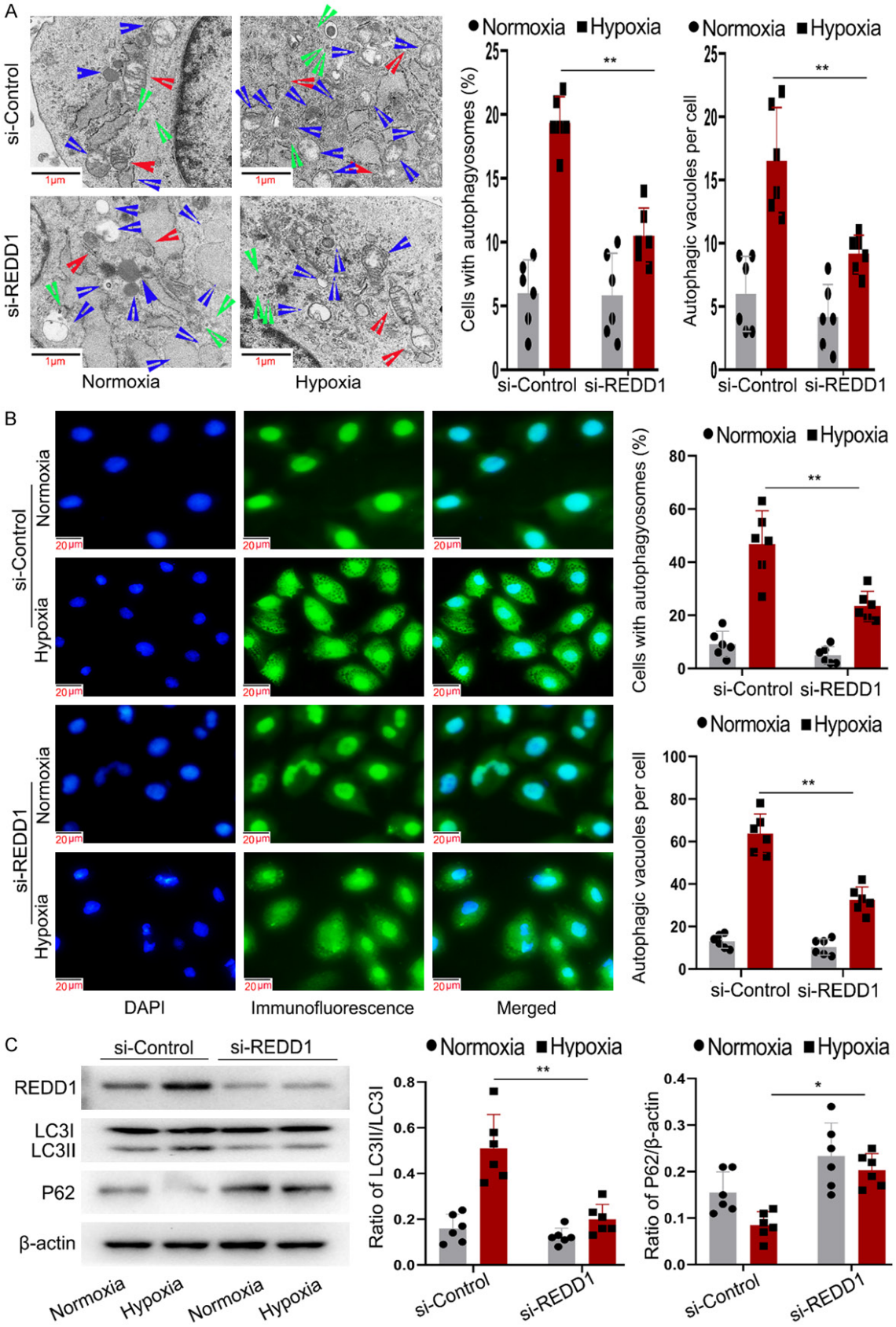
A
si-Control
si-REDD1
1μm
Normoxia
Hypoxia
Normoxia Hypoxia
Cells with autophagyosomes (%)
Autophagic vacuoles per cell
si-Control si-REDD1
**
B
si-Control
si-REDD1
Normoxia
Hypoxia
20μm
DAPI
Immunofluorescence
Merged
Cells with autophagyosomes (%)
Autophagic vacuoles per cell
C
si-Control
si-REDD1
REDD1
LC3I
LC3II
P62
β-actin
Normoxia
Hypoxia
Ratio of LC3II/LC3I
Ratio of P62/β-actin
*

Figure 6. Knockdown of REDD1 inhibits hypoxia-induced autophagy in HPASMCs. A. The percentage of cells with autophagosomes and numbers of the autophagic vacuoles per cell were quantified according to the images of the transmission electron microscope. B. Immunofluorescent staining in HPASMCs transfected with si-NC and si-REDD1 exposed to normoxia (21% Oxygen) and hypoxia (5% Oxygen). C. Brands and quantification of LC3 and P62 protein levels in each group. n=6 per group. $^{*}P$ value <0.05, $^{**}P$ value <0.01. Red arrow: mitochondria; Blue arrow: vesicles; Green arrow: dense body.

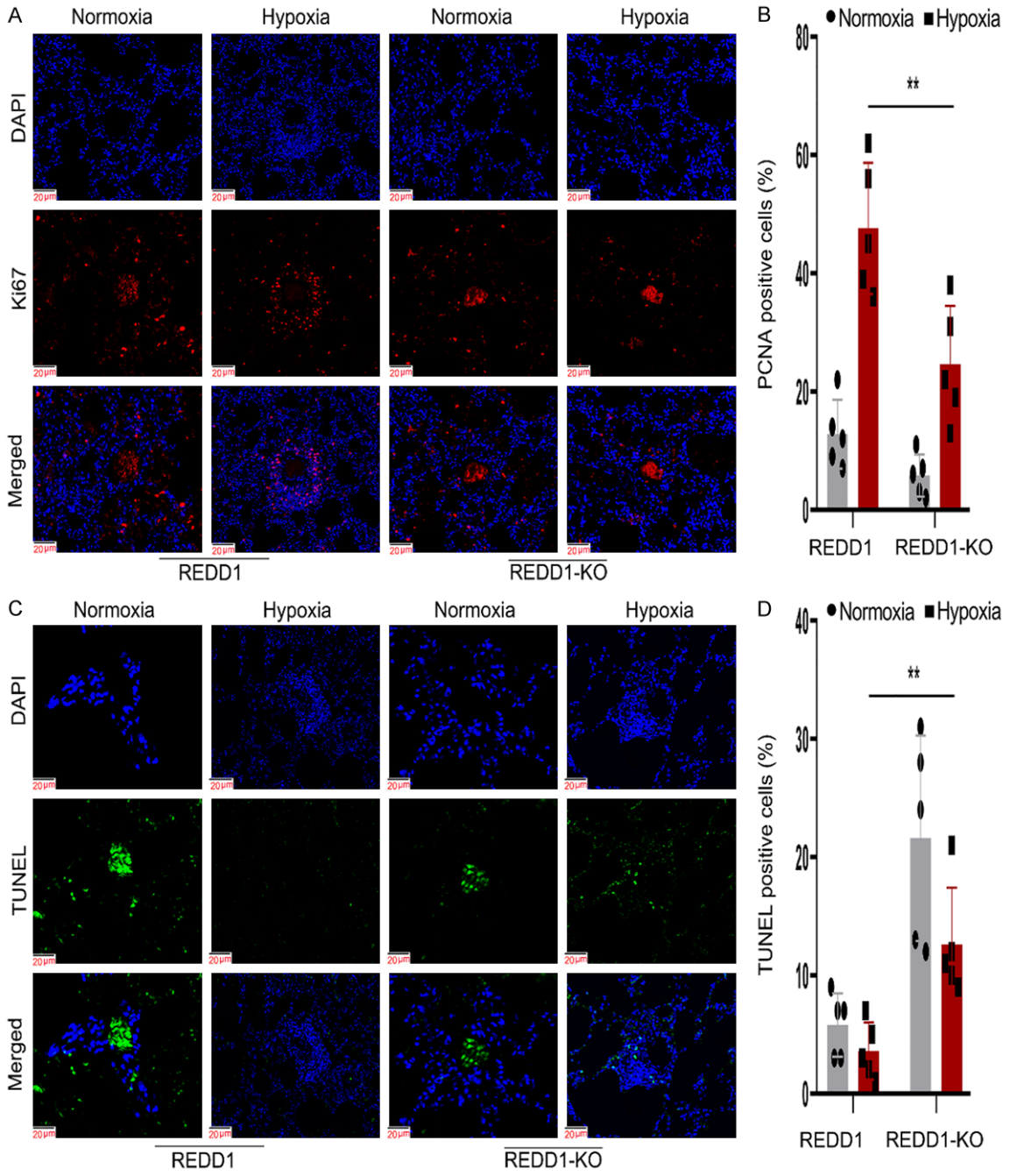

Figure 7. REDD1 deficiency results in decreased PASMCs proliferation and increased apoptosis in hypoxia rats. (A) The proliferation was estimated by of Ki67 staining. (B) Quantitation data of (A). (C) TUNEL assays were performed to observe the apoptosis and (D) Quantitation data of (C). Nuclei were stained with DAPI. n=6 per group. $^{*}P$ value <0.05, $^{**}P$ value <0.01.

fusion, increased mitochondrial ROS release, and mitochondrial membrane potential (Δψm) rise. All these changes could be reversed by inhibiting REDD1. Therefore, REDD1 may play a biological role by regulating mitochondrial homeostasis.

Under the action of external stimuli such as hypoxia, nutrient deficiency and cell senescence, the mitochondrial membrane potential in the cell decreases and depolarization occurs. When the mitochondria are severely damaged, the damaged mitochondria are cleared mainly through the autophagy pathway, thus maintaining mitochondrial homeostasis. Autophagy plays an important role in promoting cell survival and proliferation under hypoxia stress. Our previous study found that autophagy promoted the proliferation of hypoxic PASMCs and participated in the formation of hypoxic pH and pulmonary artery remodeling [10]. In addition, studies have also found that intermittent hypoxia activates autophagy by upregulating UCP2 expression in endothelial cells, leading to PH [14]. In this study, we found that hypoxic-induced autophagy significantly reduced after inhibition of REDD1 either in vivo or in vitro. Therefore, REDD1 may play a biological role in maintaining mitochondrial homeostasis of hypoxic PASMCs by activating autophagy.

It has been reported that REDD1 plays an important role in the regulation of hypoxic tolerance, proliferation, apoptosis and autophagy. Our previous studies have confirmed that hypoxia mainly promotes the proliferation and apoptosis tolerance of PASMCs by regulating mTOR to regulate and activate autophagy [15]. Meanwhile, recent studies have shown that REDD1 negatively regulates mTOR, thereby participating in a series of biological processes. In head and neck squamous cell carcinoma (HNSCC), overexpression of REDD1 inhibited mTOR activity in hypoxic environments, thereby promoting tumor cell proliferation and anchor-dependent growth [16]. It has been shown that REDD1 can inhibit mTOR and downstream p60S6K activity and regulate the proliferation of lung cancer cells [17]. Chang et al. found that inhibition of REDD1 with siRNA increased mTOR activity and resulted in decreased aggressiveness of ovarian cancer cells [18]. Recent studies have also shown that NAE enzyme inhibitors activate autophagy through the REDD1-mTOR regulatory pathway [19]. However, in our study, we found that the expression of mTOR did not change after the inhibition of REDD1. Therefore, in the hypoxia PH model, the regulation of REDD1 on autophagy may not be through the mTOR signaling pathway.

Hypoxia leads to the imbalance of PASMCs cell proliferation, apoptosis and migration, which are the main mechanisms of hypoxic pulmonary vascular remodeling [20]. Apoptosis resistance, abnormal proliferation and increased migration are common features of hypoxic PASMCs. Hypoxia is known to reduce PASMCs apoptosis through mitochondrial apoptosis or proliferation signaling pathways. Hypoxia exposure reduces the release of cytochrome C to cytosol, thereby inhibiting the apoptosis of hypoxic PASMCs. In animal models, we found that apigenin effectively promoted the mitochondrial apoptosis pathway of PASMCs and was successfully used to reverse PH pulmonary vascular remodeling. In this study, REDD1 deficiency reversed the ratio of hypoxic mitochondrial apoptosis protein Bax/Bcl2 and hypoxic-induced apoptosis resistance of PASMCs. Furthermore, hypoxic-induced migration significantly reduced. In summary, REDD1 can participate in hypoxia-induced apoptosis resistance of PASMCs cells and increase migration, thus promoting hypoxic vascular remodeling.

In conclusion, the results of this study indicate that REDD1 can maintain mitochondrial homeostasis of hypoxic PASMCs by activating autophagy, thereby inhibiting proliferation, apoptosis tolerance, migration of PASMCs, and PH progression. Although further studies are needed to reveal its clinical application, this study provides an important contribution to the establishment of a therapeutic approach for PH.

Acknowledgements

This work was supported by the National Natural Science Foundation of China (No. 81700051 and 81670048), the National Key Technology R&D Program of the 12th National Five-year Development Plan (No. 2012BAI-05B01), and the National Key Research and Development Programs of China (No. 2016-YFC1304500, 2016YFC0903600).

Disclosure of conflict of interest

None.

Address correspondence to: Yuanzhou He, Department of Respiratory Diseases, NHC Key Laboratory of Respiratory Diseases, Department of Respiratory and Critical Care Medicine, Tongji Hospital, Tongji Medical College, Huazhong University of Sciences and Technology, 1095 Jiefang Avenue, Wuhan 430030, Hubei, China. E-mail: yuanzhouhe84@163.com

References

[1] Mandras SA, Mehta HS and Vaidya A. Pulmonary hypertension: a brief guide for clinicians. Mayo Clin Proc 2020; 95: 1978-1988.

[2] Hambly N, Alawfi F and Mehta S. Pulmonary hypertension: diagnostic approach and optimal management. CMAJ 2016; 188: 804-812.

[3] Dromparis P and Michelakis ED. Mitochondria in vascular health and disease. Annu Rev Physiol 2013; 75: 95-126.

[4] Rowlands DJ. Mitochondria dysfunction: a novel therapeutic target in pathological lung remodeling or bystander? Pharmacol Ther 2016; 166: 96-105.

[5] Ryan JJ and Archer SL. Emerging concepts in the molecular basis of pulmonary arterial hypertension: part I: metabolic plasticity and mitochondrial dynamics in the pulmonary circulation and right ventricle in pulmonary arterial hypertension. Circulation 2015; 131: 1691-702.

[6] Sun XQ, Zhang R, Zhang HD, Yuan P, Wang XJ, Zhao QH, Wang L, Jiang R, Jan Bogaard H and Jing ZC. Reversal of right ventricular remodeling by dichloroacetate is related to inhibition of mitochondria-dependent apoptosis. Hypertens Res 2016; 39: 302-11.

[7] Yun SM, Woo SH, Oh ST, Hong SE, Choe TB, Ye SK, Kim EK, Seong MK, Kim HA, Noh WC, Lee JK, Jin HO, Lee YH and Park IC. Melatonin enhances arsenic trioxide-induced cell death via sustained upregulation of Redd1 expression in breast cancer cells. Mol Cell Endocrinol 2016; 422: 64-73.

[8] Dungan CM, Wright DC and Williamson DL. Lack of REDD1 reduces whole body glucose and insulin tolerance, and impairs skeletal muscle insulin signaling. Biochem Biophys Res Commun 2014; 453: 778-83.

[9] Lipina C and Hundal HS. Is REDD1 a metabolic Éminence Grise? Trends Endocrinol Metab 2016; 27: 868-880.

[10] He Y, Cao X, Guo P, Li X, Shang H, Liu J, Xie M, Xu Y and Liu X. Quercetin induces autophagy via FOXO1-dependent pathways and autophagy suppression enhances quercetin-induced apoptosis in PASMCs in hypoxia. Free Radic Biol Med 2017; 103: 165-176.

[11] Li X, He Y, Xu Y, Huang X, Liu J, Xie M and Liu X. KLF5 mediates vascular remodeling via HIF-1α in hypoxic pulmonary hypertension. Am J Physiol Lung Cell Mol Physiol 2016; 310: L299-310.

[12] Qiao S, Dennis M, Song X, Vadysirisack DD, Salunke D, Nash Z, Yang Z, Liesa M, Yoshioka J, Matsuzawa S, Shirihai OS, Lee RT, Reed JC and Ellisen LW. A REDD1/TXNIP pro-oxidant complex regulates ATG4B activity to control stress-induced autophagy and sustain exercise capacity. Nat Commun 2015; 6: 7014.

[13] Horak P, Crawford AR, Vadysirisack DD, Nash ZM, DeYoung MP, Sgroi D and Ellisen LW. Negative feedback control of HIF-1 through REDD1-regulated ROS suppresses tumorigenesis. Proc Natl Acad Sci U S A 2010; 107: 4675-80.

[14] Haslip M, Dostanic I, Huang Y, Zhang Y, Russell KS, Jurczak MJ, Mannam P, Giordano F, Erzurum SC and Lee PJ. Endothelial uncoupling protein 2 regulates mitophagy and pulmonary hypertension during intermittent hypoxia. Arterioscler Thromb Vasc Biol 2015; 35: 1166-78.

[15] Chang B, Liu G, Yang G, Mercado-Uribe I, Huang M and Liu J. REDD1 is required for RAS-mediated transformation of human ovarian epithelial cells. Cell Cycle 2009; 8: 780-6.

[16] Schneider A, Younis RH and Gutkind JS. Hypoxia-induced energy stress inhibits the mTOR pathway by activating an AMPK/REDD1 signaling axis in head and neck squamous cell carcinoma. Neoplasia 2008; 10: 1295-302.

[17] Jin HO, Seo SK, Woo SH, Kim YS, Hong SE, Yi JY, Noh WC, Kim EK, Lee JK, Hong SI, Choe TB and Park IC. Redd1 inhibits the invasiveness of non-small cell lung cancer cells. Biochem Biophys Res Commun 2011; 407: 507-11.

[18] Yang CS, Matsuura K, Huang NJ, Robeson AC, Huang B, Zhang L and Kornbluth S. Fatty acid synthase inhibition engages a novel caspase-2 regulatory mechanism to induce ovarian cancer cell death. Oncogene 2015; 34: 3264-72.

[19] Gu Y, Kaufman JL, Bernal L, Torre C, Matulis SM, Harvey RD, Chen J, Sun SY, Boise LH and Lonial S. MLN4924, an NAE inhibitor, suppresses AKT and mTOR signaling via upregulation of REDD1 in human myeloma cells. Blood 2014; 123: 3269-76.

[20] Chowdhury B, Luu AZ, Luu VZ, Kabir MG, Pan Y, Teoh H, Quan A, Sabongui S, Al-Omran M, Bhatt DL, Mazer CD, Connelly KA, Verma S and Hess DA. The SGLT2 inhibitor empagliflozin reduces mortality and prevents progression in experimental pulmonary hypertension. Biochem Biophys Res Commun 2020; 524: 50-56.

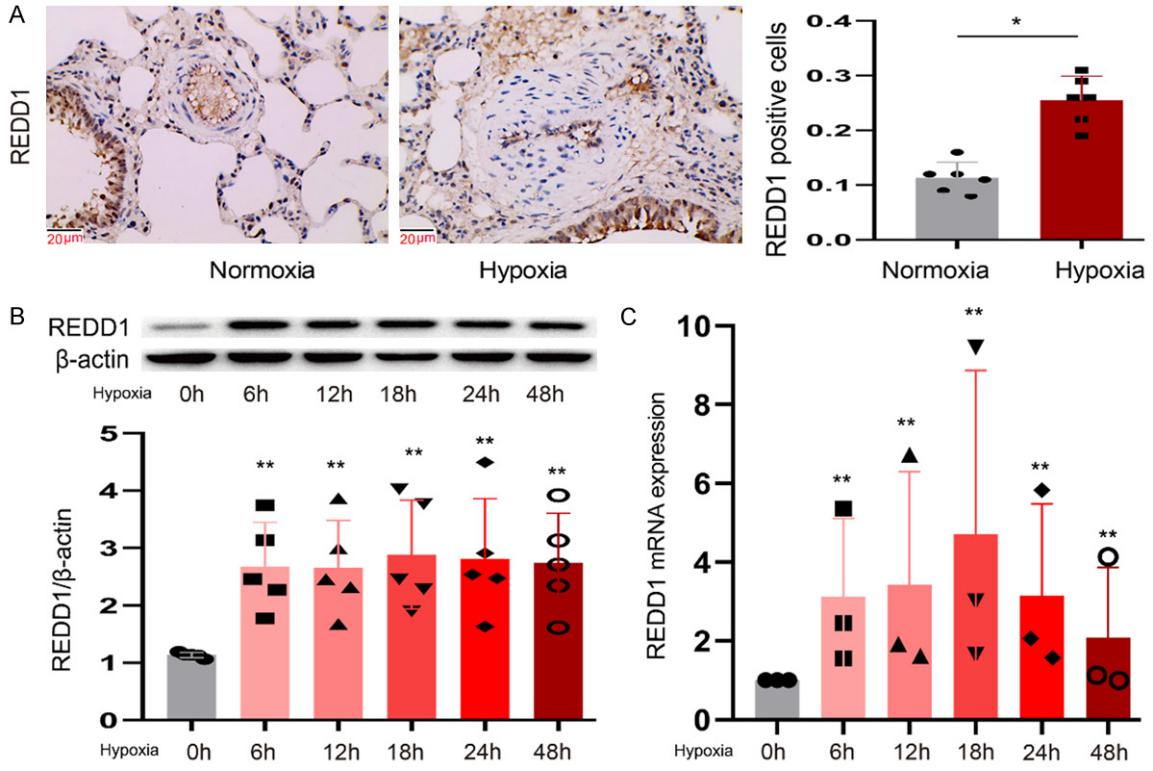

Figure S1. REDD1 is upregulated in hypoxia-induced PH rats and hypoxic HPSMCs. A. Representative images (400×) of REDD1 expression in rats exposed to normoxia (21% oxygen) or hypoxia (10% oxygen) for 4 weeks (n=6 for each group). B. Western blot analysis and quantification of REDD1 protein levels in HPASMCs with different time of hypoxia (5% oxygen), and 0 h was used as the control (n=5). C. mRNA levels of REDD1 quantified by real-time PCR in HPASMCs at different hypoxia time (n=3). $^{*}P$ value <0.05, $^{**}P$ value <0.01.

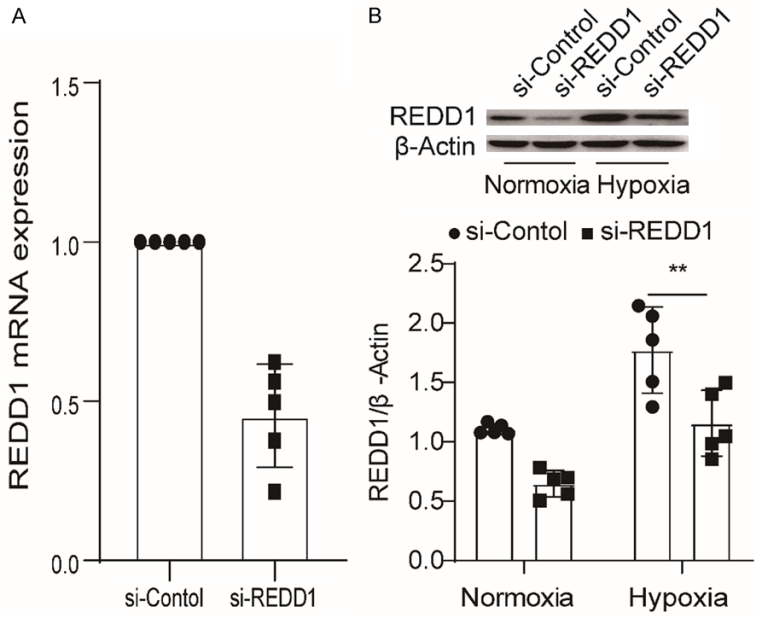

Figure S2. The efficiency of si-REDD1. A. REDD1 mRNA levels of REDD1 were analyzed in HPASMCs under normoxic and hypoxic environment (n=5). B. REDD1 protein levels were analyzed by western blot in HPASMCs transfected with si-NC and si-REDD1 exposed to normoixa or hypoxia (n=5). $^{*}P$ value <0.05, $^{**}P$ value <0.01.

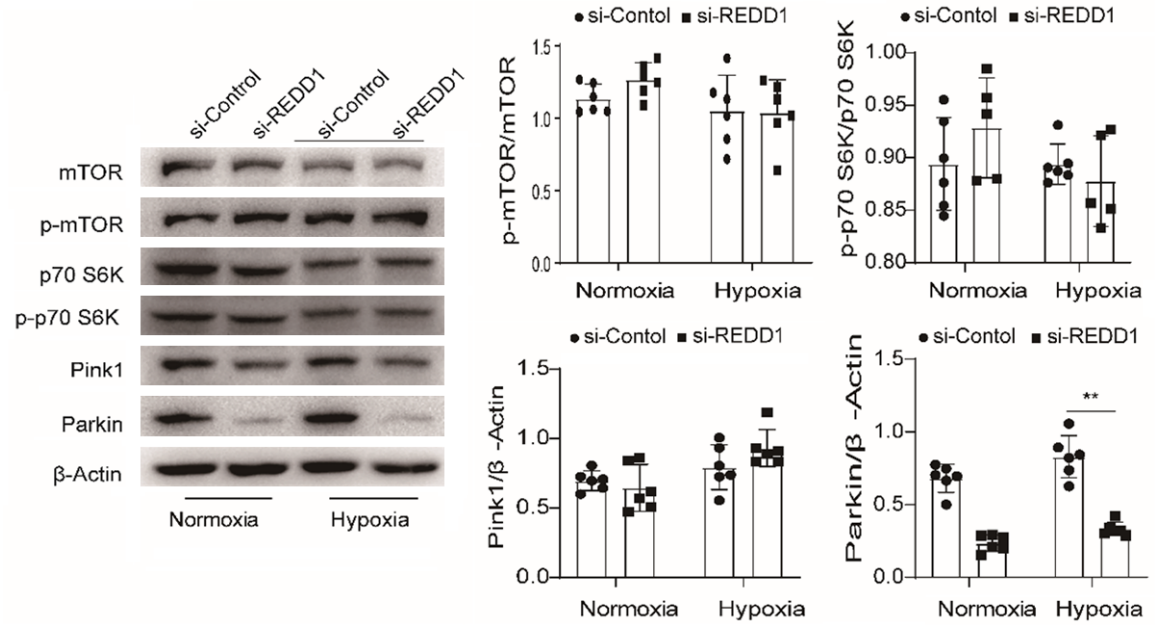

Figure S3. The effect of silencing REDD1 on classical autophagy regulatory pathways. si-REDD1 had no effects on the mTOR and Pink. However, REDD1 deletion significantly reversed the change in Parkin expression by hypoxia.

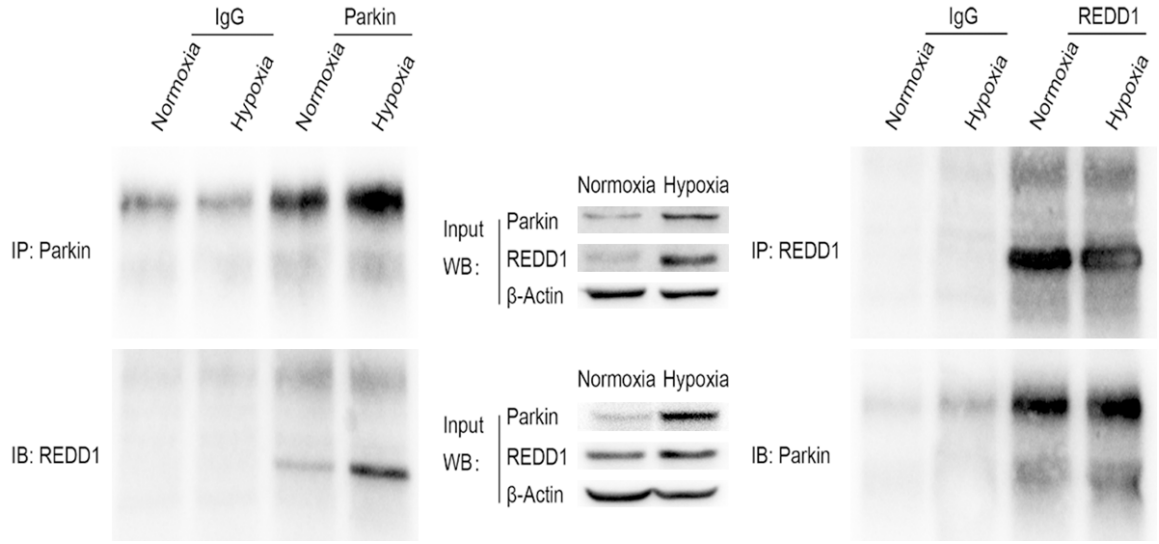

Figure S4. REDD1 and Parkin interacted directly in HPASMCs. Coimmunoprecipitation and immunoblotting detected the potential interaction between REDD1 and Parkin.

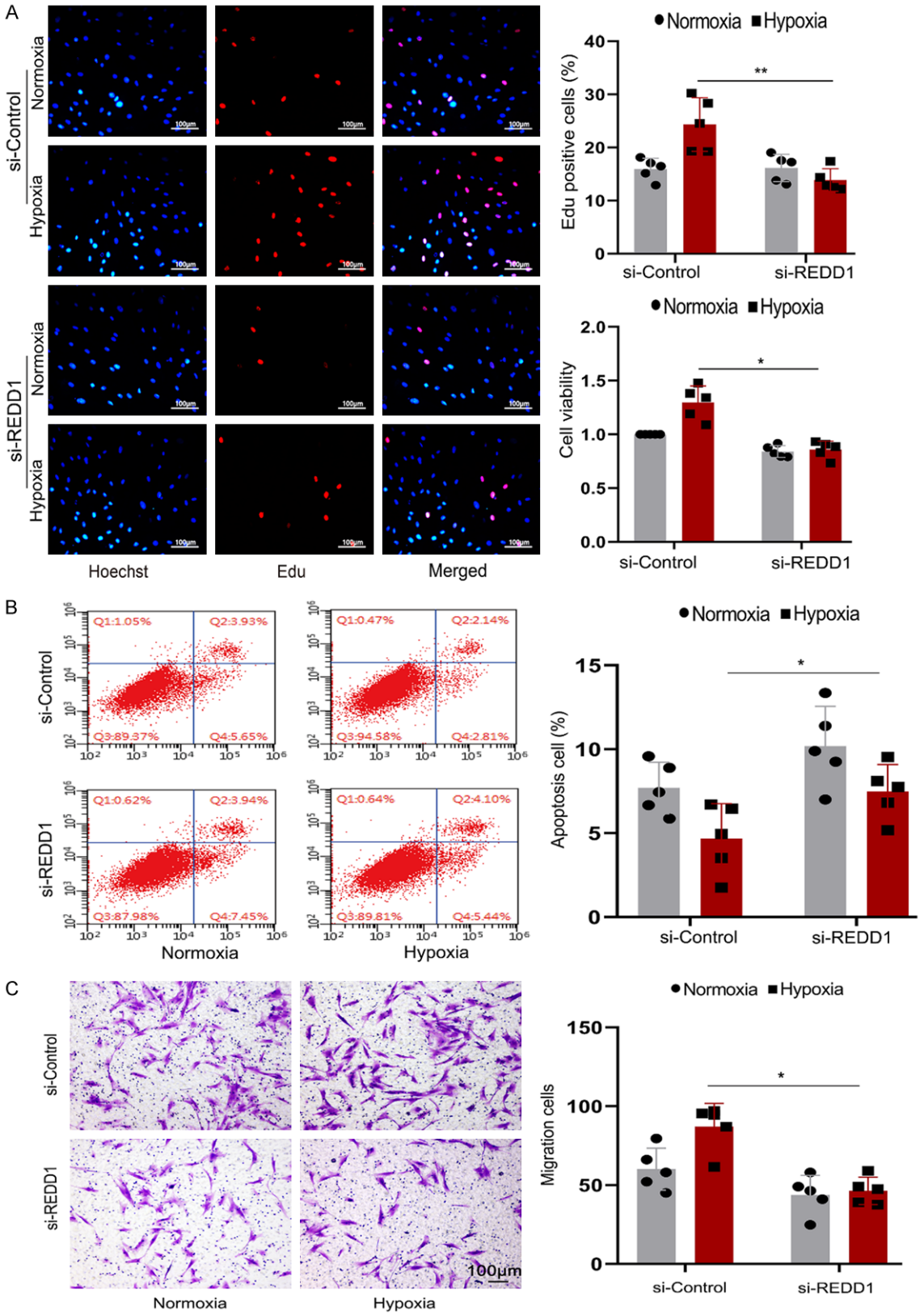

Figure S5. The influence of REDD1 knockdown on the proliferation, apoptosis and migration in HPASMCs. A. The Edu assays and CCK8 were used to detect cell proliferation and the Edu positive cells were analyzed. B. Annexin V/PI staining was applied to assess cell apoptosis, and the percentage of apoptosis cells (Annexin V positive) was shown. C. Images of cell migration were presented, and the numbers of migrated cells were counted. n=6 per group $^{*}P$ value <0.05, $^{**}P$ value <0.01.

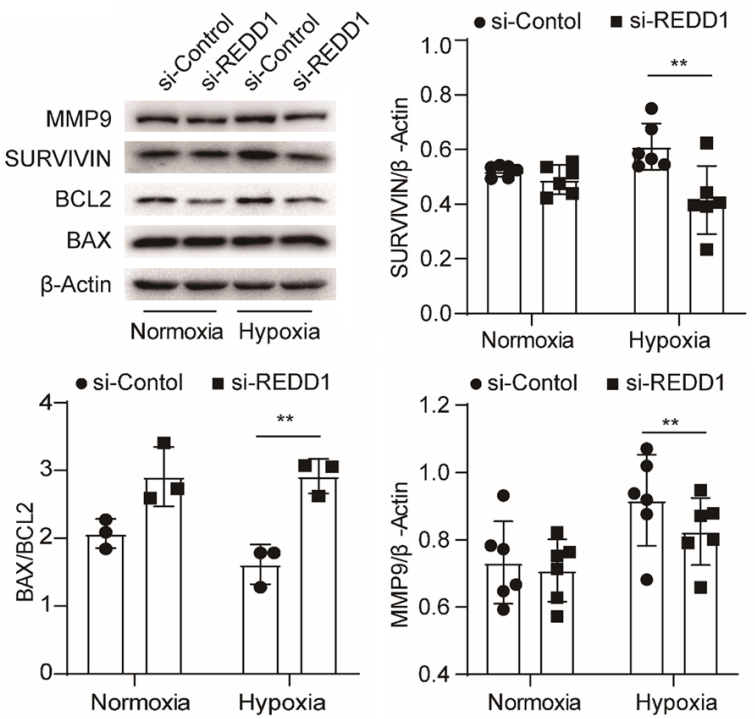

Figure S6. REDD1 regulates the expression of protein related to proliferation, apoptosis and migration in HPASMCs. The protein levels of SURVIVIN, BCL2, BAX, and MMP9 were quantified by western blot in normoxic or hypoxic HPASMCs transfected with si-NC and si-REDD1. The ratios of SURVIVIN to β-actin (n=3), BAX to BCL2 (n=6), and MMP9 to β-actin (n=6) were shown, $^{*}P$ value <0.05, $^{**}P$ value <0.01.

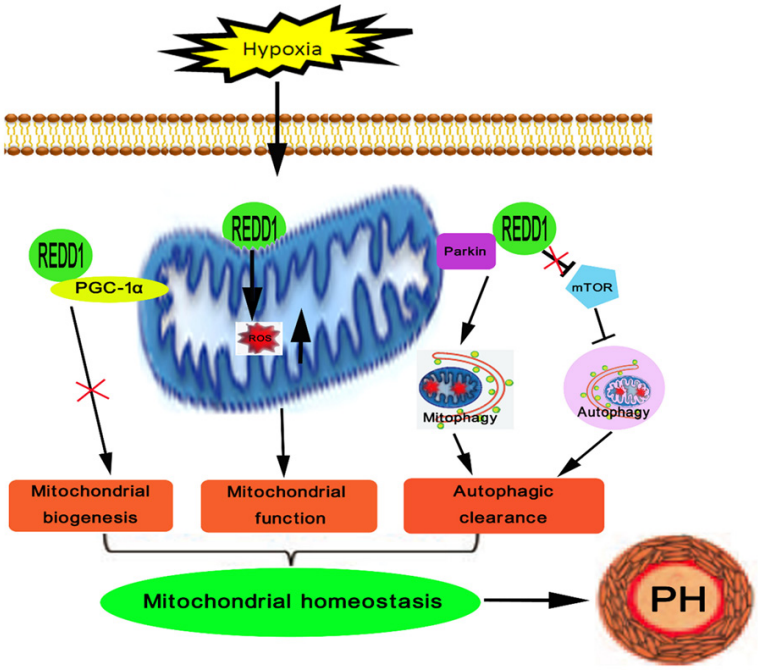

Figure S7. Graphical abstract. Graphical summary illustrating that REDD1 contributes to pulmonary hypertension via modulating mitochondria homeostasis.